

TRACKING AIRCRAFT TRAJECTORIES IN THE PRESENCE OF WIND DISTURBANCES

NIKOLAI BOTKIN AND VARVARA TUROVA*

Technische Universität München, Department of Mathematics
Boltzmannstr. 3, 85748 Garching near Munich, Germany

BARZIN HOSSEINI, JOHANNES DIEPOLDER AND FLORIAN HOLZAPFEL

Technische Universität München, Institute of Flight System Dynamics
Boltzmannstr. 15, 85748 Garching near Munich, Germany

ABSTRACT. A method of path following, utilized in the theory of position differential games as a tool for establishing theoretical results, is adopted in this paper for tracking aircraft trajectories under windshear conditions. It is interesting to note that reference trajectories, obtained as solutions of optimal control problems with zero wind, can very often be tracked in the presence of rather severe wind disturbances. This is shown in the present paper for rather realistic and highly nonlinear models of aircraft dynamics.

1. Introduction. Trajectory tracking represents an essential task for flight control systems. Under this task, it is vital to ensure that the employed methods are accurate and in particular robust against disturbances. This is especially important for critical phases of flight such as approach and landing due to navigation in crowded airspace and ground proximity. In these phases, deviations from the reference trajectory caused by disturbances can lead to catastrophic consequences. Hereby, wind represents one of the most dangerous disturbances for flight systems due to its unpredictability and heavy influence on the aircraft dynamics. Considering the criticality of the control task in the mentioned flight conditions several approaches have been investigated for this application so far. In [19] the authors propose a gamma/theta guidance law to follow trajectories derived from optimal control methods with known wind field. The authors formulate the problem in the vertical plane and illustrate the developed approach using a numerical example for the take-off phase. The study in [15] proposes an adaptive control scheme which uses the idea to control the climb rate of the aircraft in the take-off phase. This feedback control law does not require a priori knowledge of the wind field. The authors in [4] apply the method of nonlinear spatial inversion for aircraft trajectory tracking. A novel guidance scheme for the vertical plane is developed which shows improved tracking performance compared to the classical nonlinear dynamic inversion based approach. Similar to [19] an a priori estimate of the existing wind disturbance is required. The landing flight phase is considered for a two-dimensional tracking

2010 *Mathematics Subject Classification.* Primary: 49N70, 49N90; Secondary: 70Q05, 34D99.

Key words and phrases. Differential games, trajectory tracking, flight dynamics, windshear conditions, landing phase, cruise flight.

The work has been supported by the DFG grant TU427/2-2 and HO4190/8-2.

* Corresponding author: V. Turova.

problem with the ground distance to the landing point as the independent variable (instead of time). Moreover, in [16] a Lyapunov based trajectory following controller is developed for a fixed-wing UAV. It is noteworthy that the feedback controller is designed to follow a pre-defined trajectory, even in the presence of model uncertainties and unknown external disturbances. As for most robust control approaches, performance is traded against robustness in the control design.

Concerning trajectory tracking problems, it is worth mentioning a differential game-theoretic method from [11] based on direct aiming to u-stable reference trajectories. This method assumes that the following u-stability property holds. If the second player (disturbance) shows its constant control on a short time interval to the first player (pilot), the first player can always force the model to meet the trajectory at the end of this time interval. Then, if the dynamics of the model satisfy the Isaacs (saddle point) condition, an extremal aiming procedure (see [11]) enables to follow the reference trajectory without any information about the disturbance. It should be noted that the model dynamics can always be slightly relaxed to fulfill the above mentioned saddle point condition. The extremal aiming procedure proposed in [11] has been adopted in [12] for tracking trajectories of dynamic systems under time-varying unknown disturbances. This publication has given rise to many investigations towards an enhancement of the method and extension of its application area (see e.g. [17] and [13]). In particular, there has been an attempt to extend the method to the case where only a part of state variables is available for measurement (cf. [14] and [18]).

Another approach to trajectory tracking is based on introducing a guide model (or simply guide) [11]. The guide has both control and disturbance at its disposal. It chooses first a constant disturbance for the current time-sampling interval to remain close to the state of the primary model, and then it chooses a control to meet the reference trajectory at the end of the current time-sampling interval. The primary model chooses a constant control that pushes its state toward the guide, or simply copies the control of the guide. An unknown disturbance signal affects the primary model. At the beginning of the next time-sampling interval, this procedure is being repeated. It should be noted that the dynamics of the guide is, as a rule, the same as of the primary model. Therefore, the above discussed u-stability of the reference trajectory and the saddle point condition guarantee that the guide can track the reference trajectory, and the primary model remains arbitrary close to the guide if the time-sampling is sufficiently fine.

Note that such a control procedure is robust with respect to small errors in measuring the state of the primary model. In the current paper, the exact measurement of all state variables of the primary model is assumed. The paper describes the above outlined guide-based control procedure and presents nontrivial 6D examples related to aircraft control under windshear conditions. The landing phases and cruise flight are considered. The aim is to track aircraft trajectories, computed in the absence of wind disturbances, in the case where windshear is present. In this connection, it is interesting to note that an aircraft is well controllable, that is, it can return to the reference trajectory if a constant wind, known to the pilot, affects the aircraft, which is, roughly speaking, the u-stability condition.

2. Conflict control system and guide model. Consider a conflict control system (primary model)

$$\dot{x} = f(t, x, u, v), \quad t \in [t_0, \theta], \quad x \in R^n, \quad u \in P \subset R^p, \quad v \in Q \subset R^q. \quad (1)$$

Here x is the state vector, u and v are control inputs of the first (pilot) and second (wind) players, respectively. Compact sets P and Q describe constraints imposed on the control inputs. It is assumed that the function f is defined on $[t_0, \theta] \times G \times P \times Q$, where G is a sufficiently large subset of R^n . The function is bounded, continuous in all variables, and Lipschitzian in x .

Introduce the following guide model:

$$\dot{w} = f(t, w, u, v), \quad t \in [t_0, \theta], \quad w \in R^n, \quad u \in P \subset R^p, \quad v \in Q \subset R^q. \quad (2)$$

The guide model has the same dynamics as (1), but the controls u and v are now at our disposal. Moreover, at any time instant t^b , we can brake the performance of (2) and continue it from an initial state w^b , where $w^b \neq w(t^b)$.

It is assumed that the manifold to be tracked (see (25)) is a multivalued map $t \rightarrow X(t) \subset R^n$, $t \geq t_0$. Usually, $X(t)$ is of the form

$$X(t) = \{x \in R^n : [x]_r = x^{\text{ref}}(t)\}.$$

Here, $[x]_r$ is the vector consisting of the first r components of x , and $t \rightarrow x^{\text{ref}}(t) \in R^r$ is a given reference trajectory. Note that the case $r = n$ is included. In the examples below, either a reference trajectory derived from an appropriate optimal control problem (with zero wind) or a constant one will be utilized.

Our intention is to provide a discrete scheme for computing the control u on the right-hand side of system (1) such that for any instant t_i of an equidistant time sampling $t_0 < t_1 < \dots < t_i < t_{i+1} < \dots$ with $t_{i+1} - t_i = \delta$, the deviation of the solution $x(t_i)$ of (1) from the solution $w(t_i)$ of guide system (2) will be small for any admissible disturbance v in (1), if the step size δ be sufficiently small.

Given that the control in guide model will be chosen to keep the guiding trajectory maximally close to a prescribed manifold, the designed algorithm will provide tracking the reference trajectory by the primary model under unpredictable wind disturbances. The efficiency of the constructed control scheme will be demonstrated on realistic high-dimensional aircraft models, which constitutes a challenging platform for the implementation of this differential game-based approach in flight simulators.

In the control design the so-called saddle point condition in a small game [11] will be taken into account:

$$\min_{u \in P} \max_{v \in Q} \ell' f(t, x, u, v) = \max_{v \in Q} \min_{u \in P} \ell' f(t, x, u, v), \quad (3)$$

for all $\ell \in R^n$, $t \in [t_0, \theta]$, and $x \in G$. Here and in what follows, the symbol “ \prime ” denotes transposition.

It means that the following relations hold:

$$\ell' f(t, x, u^0, v) \leq \ell' f(t, x, u^0, v^0) \leq \ell' f(t, x, u, v^0),$$

where

$$u^0 = \arg \min_{u \in P} \max_{v \in Q} \ell' f(t, x, u, v), \quad v^0 = \arg \max_{v \in Q} \min_{u \in P} \ell' f(t, x, u, v).$$

If (3) does not hold in pure controls u and v , the counter controls $v(u)$ [11] of the second player discriminating the first player will be used in guide model. In this case, the relation

$$\ell' f(t, x, u^0, v(u^0)) \leq \ell' f(t, x, u^0, v^0(u^0)) \leq \ell' f(t, x, u, v^0(u)), \quad (4)$$

where

$$v^0(u) = \arg \max_{v \in Q} \ell' f(t, x, u, v),$$

will be applied to estimate the distance between the primary and guide trajectories. This relation means the existence of a saddle point in pure controls $u \in P$ of the first player and counter controls $v(u) \in Q$ of the second player.

3. Local estimate. Let $t_* \in [t_0, \theta]$. Consider the following initial value problems:

$$\dot{x} = f(t, x, u^0, v(t)), \quad x(t_*) = x_*, \tag{5}$$

$$\dot{w} = f(t, w, u(t), v^0), \quad w(t_*) = w_*. \tag{6}$$

Here $v(t)$ is an unknown admissible disturbance signal, $u(t)$ is an admissible control whose choice will be discussed later. The constant vectors u^0 and v^0 are found from the relations

$$\max_{v \in Q} (x_* - w_*)' f(t_*, x_*, u^0, v) = \min_{u \in P} \max_{v \in Q} (x_* - w_*)' f(t_*, x_*, u, v), \tag{7}$$

$$\min_{u \in P} (x_* - w_*)' f(t_*, x_*, u, v^0) = \max_{v \in Q} \min_{u \in P} (x_* - w_*)' f(t_*, x_*, u, v). \tag{8}$$

Introduce the following function (see [11, p. 65, formulas (15) and (16)]):

$$\beta(t, \delta) = \frac{1}{\lambda} \left[e^{2\lambda(t-t_*)} - 1 \right] \alpha(\delta), \tag{9}$$

where

$$\alpha(\delta) = 2[2\Lambda\delta + 1][\zeta(\delta) + \lambda\Lambda\delta] + 2\Lambda^2\delta. \tag{10}$$

The constants λ and Λ and the function $\zeta(\delta)$ are defined in [11, pp.64-65, formulas (11)-(12)]. Namely, λ and $\zeta(\delta)$ satisfy the relation

$$\|f(t_1, x_1, u, v) - f(t_2, x_2, u, v)\| \leq \lambda \|x_1 - x_2\| + \zeta(\delta) \tag{11}$$

for all $(t_{1,2}, x_{1,2}, u, v) \in [t_0, \theta] \times G \times P \times Q$ with $|t_1 - t_2| \leq \delta$, and $\zeta(\delta) \rightarrow 0$ as $\delta \rightarrow +0$. The constant Λ is the maximum of f over its definition region. Here and below the notation $\|\cdot\|$ means the Euclidean norm.

Remark 1. Note that $\alpha(\delta) \rightarrow 0$ as $\delta \rightarrow 0$. Therefore, there exists $\delta_0 > 0$ such that $\beta(t, \delta) < 1$ for all $\delta \in (0, \delta_0]$ and all $t \in [t_0, \theta]$.

It is also worth to note that $\zeta(\delta) \sim \delta$, if f is Lipschitz continuous in t . Therefore, $\beta(t, \delta)$ is of the order of δ in this case. The last claim is also true if f is time independent.

Lemma 3.1 (Lemma 2.3.1, p. 66 of [11]). *Assume that the saddle point condition (3) is true. Let $\|x_* - w_*\|^2 \leq \beta(t_*, \delta)$, $\delta \in (0, \delta_0)$. Then the following estimate holds for any choice of admissible functions $v(t)$ and $u(t)$:*

$$\|x(t) - w(t)\|^2 \leq \beta(t, \delta), \quad t \in [t_*, t_* + \delta].$$

Lemma 3.2. *Assume that the function f has the following structure: $f(t, x, u, v) = f_1(t, x, u) + f_2(t, x, v)$. Then the saddle point condition holds. Moreover, if the vector u^0 in (5) is replaced with the control $u(t)$ from (6), then the local estimate from Lemma 3.1 holds for any choice of admissible functions $u(t)$ and $v(t)$.*

Proof. The following formulas are true:

$$x(t) = x_* + \int_{t_*}^t f(\xi, x(\xi), u(\xi), v(\xi)) d\xi,$$

$$w(t) = w_* + \int_{t_*}^t f(\xi, w(\xi), u(\xi), v^0) d\xi.$$

It is easy to check that

$$\begin{aligned}
x(t) - w(t) &= x_* - w_* \\
&+ \int_{t_*}^t [f(t_*, x_*, u(\xi), v(\xi)) - f(t_*, x_*, u(\xi), v^0)] d\xi \\
&+ \int_{t_*}^t [f(\xi, x_*, u(\xi), v(\xi)) - f(t_*, x_*, u(\xi), v(\xi))] d\xi \quad \sim o(t - t_*) \\
&+ \int_{t_*}^t [f(t_*, x_*, u(\xi), v^0) - f(\xi, x_*, u(\xi), v^0)] d\xi \quad \sim o(t - t_*) \\
&+ \int_{t_*}^t [f(\xi, x(\xi), u(\xi), v(\xi)) - f(\xi, x_*, u(\xi), v(\xi))] d\xi \quad \sim o(t - t_*) \\
&+ \int_{t_*}^t [f(\xi, w_*, u(\xi), v^0) - f(\xi, w(\xi), u(\xi), v^0)] d\xi, \quad \sim o(t - t_*) \\
&+ \int_{t_*}^t [f(\xi, x_*, u(\xi), v^0) - f(\xi, w_*, u(\xi), v^0)] d\xi. \quad \sim (t - t_*)\lambda\|x_* - w_*\|
\end{aligned}$$

where λ is defined by formula (11). Therefore,

$$\begin{aligned}
\|x(t) - w(t)\|^2 &\leq (1 + \lambda(t - t_*))\|x_* - w_*\|^2 \\
&+ \int_{t_*}^t (x_* - w_*)' [f(t_*, x_*, u(\xi), v(\xi)) - f(t_*, x_*, u(\xi), v^0)] d\xi + o(t - t_*). \quad (12)
\end{aligned}$$

Obviously,

$$(x_* - w_*)' f(t_*, x_*, u(\xi), v(\xi)) \leq (x_* - w_*)' f(t_*, x_*, u(\xi), v^0), \quad (13)$$

for all $u(\xi)$ and $v(\xi)$, which is equivalent to the inequality

$$(x_* - w_*)' f_2(t_*, x_*, v(\xi)) \leq (x_* - w_*)' f_2(t_*, x_*, v^0) \quad (14)$$

holding for all $v(\xi)$.

Exactly estimating $o(t - t_*)$ in (12) (see Lemma 2.3.1, p. 68 of [11]) proves the lemma. \square

Lemma 3.3. *Assume that the saddle point condition does not hold, i.e.*

$$\min_{u \in P} \max_{v \in Q} (x_* - w_*)' f(t_*, x_*, u, v) > \max_{v \in Q} \min_{u \in P} (x_* - w_*)' f(t_*, x_*, u, v). \quad (15)$$

For any constant vector $u \in P$, let $v^0(u)$ be a maximizer in the maximization problem $\max_{v \in Q} (x_* - w_*)' f(t_*, x_*, u, v)$. If the vector u^0 in (5) is replaced with the control $u(t)$ from (6), and the vector v^0 in (6) is replaced with $v^0(u(t))$, then the local estimate from Lemma 3.1 holds for any choice of admissible functions $u(t)$ and $v(t)$.

Proof. We have:

$$\begin{aligned}
x(t) &= x_* + \int_{t_*}^t f(\xi, x(\xi), u(\xi), v(\xi)) d\xi, \\
w(t) &= w_* + \int_{t_*}^t f(\xi, w(\xi), u(\xi), v^0(u(\xi))) d\xi.
\end{aligned}$$

Hence,

$$x(t) - w(t) = x_* - w_*$$

$$\begin{aligned}
 & + \int_{t_*}^t [f(t_*, x_*, u(\xi), v(\xi)) - f(t_*, x_*, u(\xi), v^0(u(\xi)))] d\xi \\
 & + \int_{t_*}^t [f(\xi, x_*, u(\xi), v(\xi)) - f(t_*, x_*, u(\xi), v(\xi))] d\xi \quad \sim o(t - t_*) \\
 & + \int_{t_*}^t [f(t_*, x_*, u(\xi), v^0(u(\xi))) - f(\xi, x_*, u(\xi), v^0(u(\xi)))] d\xi \quad \sim o(t - t_*) \\
 & + \int_{t_*}^t [f(\xi, x(\xi), u(\xi), v(\xi)) - f(\xi, x_*, u(\xi), v(\xi))] d\xi \quad \sim o(t - t_*) \\
 & + \int_{t_*}^t [f(\xi, w_*, u(\xi), v^0(u(\xi))) - f(\xi, w(\xi), u(\xi), v^0(u(\xi)))] d\xi, \quad \sim o(t - t_*) \\
 & + \int_{t_*}^t [f(\xi, x_*, u(\xi), v^0(u(\xi))) - f(\xi, w_*, u(\xi), v^0(u(\xi)))] d\xi. \quad \sim (t - t_*)\lambda\|x_* - w_*\|
 \end{aligned}$$

Therefore,

$$\begin{aligned}
 \|x(t) - w(t)\|^2 & \leq (1 + \lambda(t - t_*))\|x_* - w_*\|^2 \\
 & + \int_{t_*}^t (x_* - w_*)' [f(t_*, x_*, u(\xi), v(\xi)) - f(t_*, x_*, u(\xi), v^0(u(\xi)))] d\xi + o(t - t_*).
 \end{aligned} \tag{16}$$

The term $o(t - t_*)$ in (16) is estimated as in Lemma 2.3.1 (p. 68 of [11]) with the difference that, instead of the saddle point condition (3), the relation (15) is used.

Finally, applying the inequality

$$(x_* - w_*)' f(t_*, x_*, u(\xi), v(\xi)) \leq (x_* - w_*)' f(t_*, x_*, u(\xi), v^0(u(\xi))), \tag{17}$$

which holds for all $u(\xi)$ and $v(\xi)$, proves the assertion of Lemma 3.3. \square

4. Global estimate for discrete-time control scheme.

Assume that an equidistant time sampling $t_0 < t_1 < \dots < t_i < t_{i+1} < \dots$ is chosen, and $t_{i+1} - t_i = \delta$ for all i .

4.1. The case of general saddle point condition. Consider the case of Lemma 3.1, where the saddle point condition holds. Let $v^{(i)}(t)$ and $u^{(i)}(t)$ be arbitrary admissible disturbances and controls affecting the primary and guide models, respectively, on time intervals $[t_i, t_{i+1}]$, $i = 0, 1, \dots$, cf. (5) and (6). Define trajectories of the models on each time interval $[t_i, t_{i+1}]$ as follows:

$$\dot{x} = f(t, x, u^{0(i)}, v^{(i)}(t)), \quad \dot{w} = f(t, w, u^{(i)}(t), v^{0(i)}), \tag{18}$$

where the vectors $u^{0(i)}$ and $v^{0(i)}$ are defined by the relations

$$\max_{v \in Q} \ell'_i f(t_i, x(t_i), u^{0(i)}, v) = \min_{u \in P} \max_{v \in Q} \ell'_i f(t_i, x(t_i), u, v), \tag{19}$$

$$\min_{u \in P} \ell'_i f(t_i, x(t_i), u, v^{0(i)}) = \max_{v \in Q} \min_{u \in P} \ell'_i f(t_i, x(t_i), u, v), \tag{20}$$

with $l_i = x(t_i) - w(t_i)$. The following lemma is true.

Lemma 4.1 (Estimate (16), p. 73 of [11]). *If $w(t_0) = x(t_0)$, then the following estimate holds:*

$$\|x(t) - w(t)\|^2 \leq \beta(t, \delta), \quad \delta \in (0, \delta_0), \quad t \in [t_i, t_{i+1}], \quad i = 0, 1, \dots \tag{21}$$

Thus, trajectories $x(t)$ and $w(t)$ track each other independently on the choice of admissible inputs $v^{(i)}(t)$ and $u^{(i)}(t)$, $i = 0, 1, \dots$.

Proof. The proof is performed using Lemma 3.1 (local estimate) and mathematical induction.

For $i = 0$ we have $\|x(t_0) - w(t_0)\|^2 = 0 = \beta(t_0, \delta)$, which means that the assertion of lemma is true. Assume that the estimate (21) holds for some $i = k > 0$, i.e. $\|x(t) - w(t)\|^2 \leq \beta(t, \delta)$, $\delta \in (0, \delta_0)$, $t \in [t_k, t_{k+1}]$. Then the conditions of Lemma 3.1 are satisfied for t_{k+1} , which implies the fulfillment of (21) for all $i > 0$. \square

Remark 2. Note that $\beta(t, \delta)$ exponentially grows with $t - t_0$, and, therefore, the trajectories may diverge with time. To correct this effect, the following trick may be used. If $\|x(t_i) - w(t_i)\|^2 > \epsilon_0$ for the current index i , then $w(t_i)$ will be forcibly pushed to the vector $x(t_i)$. I.e., it will be forcibly set $w(t_i) = x(t_i)$. This is not a violation of reality because the guide model (2) is completely at our disposal.

4.2. The case of additively separable controls. Consider the case of Lemma 3.2, where $f(t, x, u, v) = f_1(t, x, u) + f_2(t, x, v)$. Let $v^{(i)}(t)$ and $u^{(i)}(t)$ be arbitrary admissible disturbances and controls affecting the primary and guide model, respectively, on time intervals $[t_i, t_{i+1}]$, $i = 0, 1, \dots$, cf. (5) and (6). Define trajectories of the models on each time interval $[t_i, t_{i+1}]$ as follows:

$$\dot{x} = f(t, x, u^{(i)}(t), v^{(i)}(t)), \quad \dot{w} = f(t, w, u^{(i)}(t), v^{0(i)}), \quad (22)$$

where the vectors $v^{0(i)}$ are defined in the same way as in (20), and the primary model uses the same control $u^{(i)}(t)$ as the guide one.

Then, all the conditions of Lemma 3.2 are satisfied and the local estimate from Lemma 3.1 is true, which implies the fulfillment of the estimate (21) for all admissible disturbances and controls, $v^{(i)}(t)$ and $u^{(i)}(t)$, $i = 0, 1, \dots$.

4.3. The case of absence of the saddle point condition. Consider the case of Lemma 3.3, where the saddle point condition does not hold. Let $v^{(i)}(t)$ and $u^{(i)}(t)$ be arbitrary admissible disturbances and controls affecting the primary and guide model, respectively, on time intervals $[t_i, t_{i+1}]$, $i = 0, 1, \dots$. Define trajectories of the models on each time interval $[t_i, t_{i+1}]$ as follows:

$$\dot{x} = f(t, x, u^{(i)}(t), v^{(i)}(t)), \quad \dot{w} = f(t, w, u^{(i)}(t), v^{0(i)}(u^{(i)}(t))), \quad (23)$$

where the function $u \rightarrow v^{0(i)}(u)$ is given by the relation

$$(x(t_i) - w(t_i))' f(t_i, x(t_i), u, v^{0(i)}(u)) = \max_{v \in Q} (x(t_i) - w(t_i))' f(t_i, x(t_i), u, v).$$

Thus, the primary model copies the control $u^{(i)}(t)$ of the guide one, and the guide model uses the counter disturbance $v^{0(i)}(u^{(i)}(t))$. Then, all the conditions of Lemma 3.3 hold and the local estimate from Lemma 3.1 is true, which implies the fulfillment of the estimate (21) for all admissible disturbances and controls, $v^{(i)}(t)$ and $u^{(i)}(t)$, $i = 0, 1, \dots$.

5. Choice of functions $v^{(i)}(t)$ and $u^{(i)}(t)$ on each time-sampling interval.

Functions $v^{(i)}(t)$, $i = 0, 1, \dots$, affecting the primary model, represent the time realization of external disturbances, and, therefore, they are not at our disposal.

Nevertheless, in simulations, these functions may be chosen from the condition of extremal repulsion from the manifold to be tracked. That is,

$$v^{(i)}(t) \equiv v^{(i)} = \arg \max_{v \in Q} (x(t_i) - \hat{x}[x(t_i), X(t_i)])' f(t_i, x(t_i), u^{0(i)}, v), \quad t \in [t_i, t_{i+1}), \tag{24}$$

where $\hat{x}[x, X]$ denotes the closest point of X to x . Here it is assumed that the saddle point condition holds, and $u^{0(i)}$ is chosen according to (19).

A function $u^{(i)}(t)$, which plays a role of control in the guide model on the time interval $[t_i, t_{i+1})$, is chosen to minimize the deviation of the guide model from the manifold at t_{i+1} , that is, to solve the problem

$$\text{dist} \left(w(t_{i+1}), X(t_{i+1}) \right) \rightarrow \min \tag{25}$$

under the condition that the disturbance $v^{0(i)}$, or counter disturbance $v^{0(i)}(u^{(i)}(t))$, is used in the guide model on the interval $[t_i, t_{i+1})$. Numerically, the function $u^{(i)}(t)$ can be searched as a step function with three values, that is,

$$u^{(i)}(t) = \begin{cases} u_1, & t \in [t_i, t_i + \delta/3), \\ u_2, & t \in [t_i + \delta/3, t_i + 2\delta/3), \\ u_3, & t \in [t_i + 2\delta/3, t_i + \delta). \end{cases} \tag{26}$$

Thus, the minimization in (25) runs over all possible combinations of u_1, u_2, u_3 .

Numerical simulations show that the ansatz (26) is not effective because the interval $[t_i, t_{i+1})$ is too small, so that the minimizing control $u^{(i)}(t)$ switches very often and does not show the direction of optimal shift. To stabilize it, the following heuristic trick is used. A relatively large time step length $\tau > \delta$ (for example, $\delta = 0.005$ s and $\tau = 0.05$ s) is chosen. The minimization problem

$$\text{dist} \left(w(t_i + 3\tau), X(t_i + 3\tau) \right) \rightarrow \min_{u^{(i)}(\cdot)} \tag{27}$$

is considered, and the following ansatz is used for the minimization:

$$u^{(i)}(t) = \begin{cases} u_1, & t \in [t_i, t_i + \tau), \\ u_2, & t \in [t_i + \tau, t_i + 2\tau), \\ u_3, & t \in [t_i + 2\tau, t_i + 3\tau). \end{cases} \tag{28}$$

The disturbances $v^{0(i)}$, or counter disturbance $v^{0(i)}(u^{(i)}(t))$, is now used on the interval $[t_i, t_i + 3\tau)$. After finding a minimizing triple u_1, u_2, u_3 , the first vector, u_1 , is used as control on the interval $[t_i, t_{i+1})$.

Remark 3. Note that the ansatz (27), (28) can be reduced to the two-interval one:

$$\text{dist} \left(w(t_i + 2\tau), X(t_i + 2\tau) \right) \rightarrow \min_{u^{(i)}(\cdot)}, \tag{29}$$

$$u^{(i)}(t) = \begin{cases} u_1, & t \in [t_i, t_i + \tau), \\ u_2, & t \in [t_i + \tau, t_i + 2\tau), \end{cases} \tag{30}$$

enlarging the step length τ . Numerical experiments show a good control quality in this case.

A basic prototype algorithm for the tracking procedure using the choice of functions described in this section is provided in Alg. 1. Observe that the primary model copies the control of the guide and uses an external disturbance $v^{(i)}$ which is not at our disposal. The value of this external disturbance depends on the application under consideration and is represented by the wind velocity in the context of the aircraft trajectory tracking problem. For testing purposes it may be chosen based on the condition of extremal repulsion (cf. (24)) or other disturbance models (e.g. the Dryden wind turbulence model used in cf. Section 6.1). It is important to note that if the minimization and maximization operators are evaluated using values from a grid for the admissible controls and disturbances each step of the algorithm requires a finite number of operations.

Algorithm 1 Tracking

```

1: procedure TRACKING( $X, \delta, t_0, \theta, x_0, Q, P, \epsilon_0$ )  $\triangleright$  Prototype tracking procedure
2:    $x^0 \leftarrow x_0$ 
3:    $w^0 \leftarrow x_0$ 
4:    $i \leftarrow 0$ 
5:   while  $i\delta < \theta$  do
6:      $t_i \leftarrow t_0 + i\delta$ 
7:     if  $\|x^i - w^i\|^2 > \epsilon_0$  then
8:        $w^i \leftarrow x^i$   $\triangleright$  reset  $w$ , see Remark 2
9:     end if
10:     $v^{0(i)} \leftarrow \arg \max_{v \in Q} \min_{u \in P} (x^i - w^i)' f(t_i, x^i, u, v)$   $\triangleright$  cf. (20)
11:     $u_1^{(i)} \leftarrow \arg \min_{u(\cdot)} \text{dist}(w(t_i + \delta), X(t_i + \delta))$   $\triangleright$  alternatively use (27) or (29)
12:     $v^{(i)} \leftarrow \text{getDisturbance}(\cdot)$   $\triangleright$  get external disturbance (e.g. using (24))
13:     $w^{i+1} \leftarrow w^i + \delta f(t_i, w^i, u_1^{(i)}, v^{0(i)})$   $\triangleright$  move  $w$  using  $u_1^{(i)}$  and  $v^{0(i)}$ 
14:     $x^{i+1} \leftarrow x^i + \delta f(t_i, x^i, u_1^{(i)}, v^{(i)})$   $\triangleright$  move  $x$  using  $u_1^{(i)}$  and disturbance  $v^{(i)}$ 
15:     $i \leftarrow i + 1$ 
16:  end while
17: end procedure

```

6. Examples.

6.1. Tracking a landing trajectory. A nonlinear point mass model of the Boeing 707 jet is under consideration. The model structure is described in Section 8 (the appendix). The derivation is based on data provided in [5] for the holding flight phase. The state vector of the aircraft model is defined as $x = [V_K, \gamma_K, \chi_K, x_N, y_N, z_N]'$ including the kinematic velocity V_K , the kinematic flight path angle γ_K , the kinematic course angle χ_K , and the aircraft position states (x_N, y_N, z_N) denoted in a local frame. The control vector $u = [\alpha_K, \mu_K, \delta_T]'$ contains the kinematic angle of attack α_K , the kinematic bank angle μ_K , and the thrust setting δ_T . The wind disturbance vector has three components $v = [W_x, W_y, W_z]'$ given in the North-East-Down (NED) frame. The wind disturbances and the controls are subject to box constraints:

$$\begin{aligned}
 |\alpha_K| &\leq 15 \text{ deg}, & |\mu_K| &\leq 15 \text{ deg}, & \delta_T &\in [0, 1], \\
 |W_x| &\leq 10 \text{ m/s}, & |W_y| &\leq 10 \text{ m/s}, & |W_z| &\leq 5 \text{ m/s}.
 \end{aligned}
 \tag{31}$$

The reference trajectory $x^{\text{ref}}(t)$ is obtained in the absence of wind disturbances (i.e. $v \equiv 0$) from the numerical solution of an appropriate optimal control problem. At the initial point of the trajectory the following boundary conditions for this optimal control problem are defined for the position, velocity, and flight path angles:

$$\begin{aligned}(x_N)_{\text{initial}} &= 0 \text{ m}, \\(y_N)_{\text{initial}} &= 0 \text{ m}, \\(z_N)_{\text{initial}} &= -400 \text{ m}, \\(V_K)_{\text{initial}} &= 110 \text{ m/s}, \\(\gamma_K)_{\text{initial}} &= 0 \text{ deg}, \\(\chi_K)_{\text{initial}} &= 0 \text{ deg}.\end{aligned}\tag{32}$$

Similarly, the final boundary conditions are represented by the landing position and constraints on the terminal velocity and the flight path angles:

$$\begin{aligned}(x_N)_{\text{landing}} &\approx 14985 \text{ m}, \\(y_N)_{\text{landing}} &\approx 65 \text{ m}, \\(z_N)_{\text{landing}} &\approx -20 \text{ m}, \\(V_K)_{\text{landing}} &\in [70, 100] \text{ m/s}, \\(\gamma_K)_{\text{landing}} &\approx 0 \text{ deg}, \\(\chi_K)_{\text{landing}} &\approx 0 \text{ deg}.\end{aligned}\tag{33}$$

The following cost function J is used for the optimal control problem

$$J = \int_{t_0}^{t_{\text{landing}}} \gamma_K dt,\tag{34}$$

which supports monotonicity of the landing trajectory.

This optimal control problem is solved using a direct method (cf. [1]). Under this approach the continuous time optimal control problem is transcribed into a nonlinear programming (NLP) problem of the following form:

$$\begin{aligned}\underset{z}{\text{minimize}} & \quad F(z) \\ \text{subject to} & \\ h(z) &= 0, \\ g(z) &\leq 0.\end{aligned}\tag{35}$$

In the transcribed problem formulation, z is a vector containing the optimization variables, $F(z)$ represents the scalar cost function, $h(z)$ collects all equality constraints, and $g(z)$ collects all inequality constraints. In case of a full discretization, which is used in this study, z collects variables for the inputs u and the states x corresponding to each discrete time point $t_k, k = 0, \dots, m$. In this paper, the number of discrete points on the equidistant time grid is set to $m = 5000$. The trapezoidal collocation method is employed to discretize the model dynamics which yields equality constraints of the following form:

$$0 = x_{k+1} - x_k - \frac{t_{k+1} - t_k}{2} (f(u_k, x_k) + f(u_{k+1}, x_{k+1})), \quad k = 0, \dots, m - 1.\tag{36}$$

Note that equality and inequality constraints related to the boundary conditions can be directly considered using the state and control variables at the discretization

time points. For all numerical examples the optimal control toolbox *Falcon.m*¹ is used to model the optimal control problem and the resulting NLP (35) is solved with the interior point solver Ipopt [21].

It is numerically proven that the saddle point condition holds for this aircraft model, so that the control scheme corresponds to Subsection 4.1. The saddle point condition was tested on the reference trajectory by evaluation of the min max and max min operators (cf. Eq. (3)) and comparing the results. The choice of the controls $u^{(i)}(t)$ in the guide model has been implemented according to the ansatz (29) and (30). Regarding the implementation of Alg. 1 for this particular example the controls are determined in two sequential steps. First, the thrust command is determined by tracking the reference velocity. From an aircraft control perspective this approach represents a natural strategy considering the fact that the thrust command can be used for acceleration and deceleration of the system. In a second step the angle of attack and the bank angle commands are determined using all reference states. Disturbances are simulated using a Dryden turbulence model outlined in Subsection 8.2.

The time step lengths are chosen as: $\delta = 0.005$ s and $\tau = 0.1$ s. Resetting of the state vector of the guide model (see Remark 2) is performed with the threshold ϵ_0 equal to 0.01. It is noteworthy, that for the simulations the covered distance x_N is used instead of time, observing that $dx/dt = dx/dx_N \cdot dx_N/dt$ and $dx_N/dt \geq const > 0$. These simulations are performed on the interval $x_N \in [0, 14887]$ m with a runtime of about 100 s using an OMP parallelization over 11 threads.

The simulation results are depicted in Figures 1-10. Figures 1-5 correspond to the characteristic value of 30 m/s in the Dryden model, whereas Figures 6-10 show numerical results for the characteristic value of 45 m/s. Additionally, the absolute values of the deviation between the reference states and aircraft states are presented in the lower plots of Figures 2-4 and Figures 7-9.

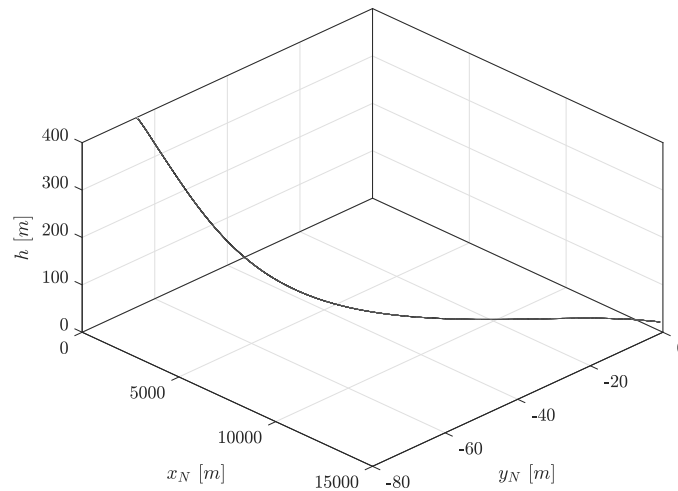


FIGURE 1. Tracking of the landing trajectory in the case of a Dryden disturbance model with the characteristic value of 30 m/s. The black line presents the aircraft motion, and the grey line shows the reference trajectory.

¹<http://www.falcon-m.com>

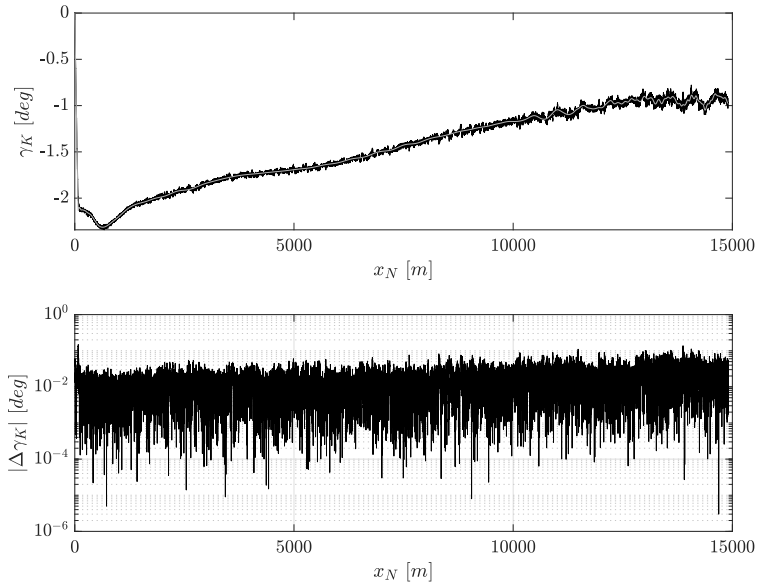


FIGURE 2. The angle γ_K [deg] in the case of a Dryden disturbance model with the characteristic value of 30 m/s. In the upper plot the black line corresponds to the aircraft motion, and the grey line stands for the reference trajectory. The solid line in the lower plot shows the absolute tracking error using a semi-logarithmic scale.

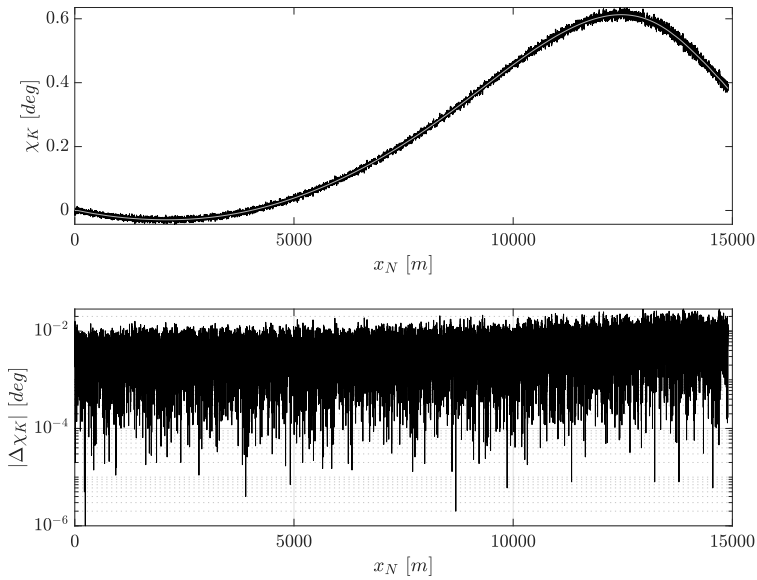


FIGURE 3. The angle χ_K [deg] in the case of a Dryden disturbance model with the characteristic value of 30 m/s. In the upper plot the black line corresponds to the aircraft motion, and the grey line stands for the reference trajectory. The solid line in the lower plot shows the absolute tracking error using a semi-logarithmic scale.

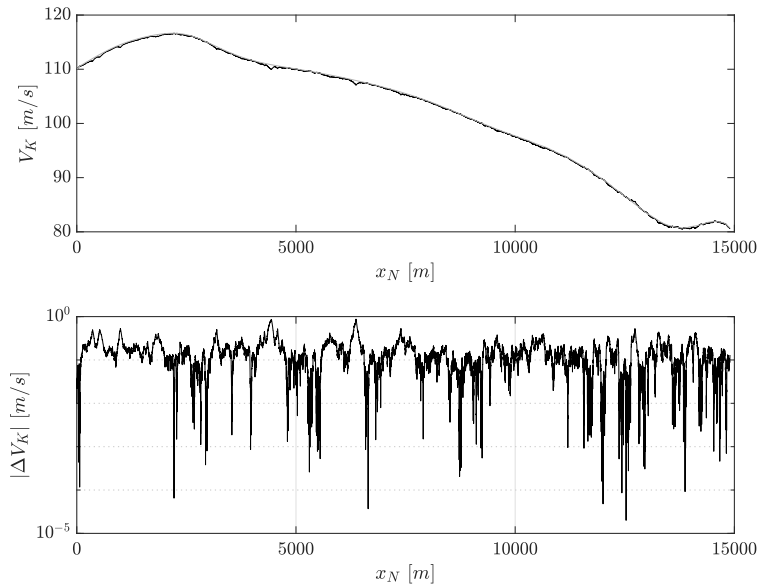


FIGURE 4. The velocity V_K [m/s] in the case of a Dryden disturbance model with the characteristic value of 30 m/s. In the upper plot the black line corresponds to the aircraft motion, and the grey line stands for the reference trajectory. The solid line in the lower plot shows the absolute tracking error using a semi-logarithmic scale.

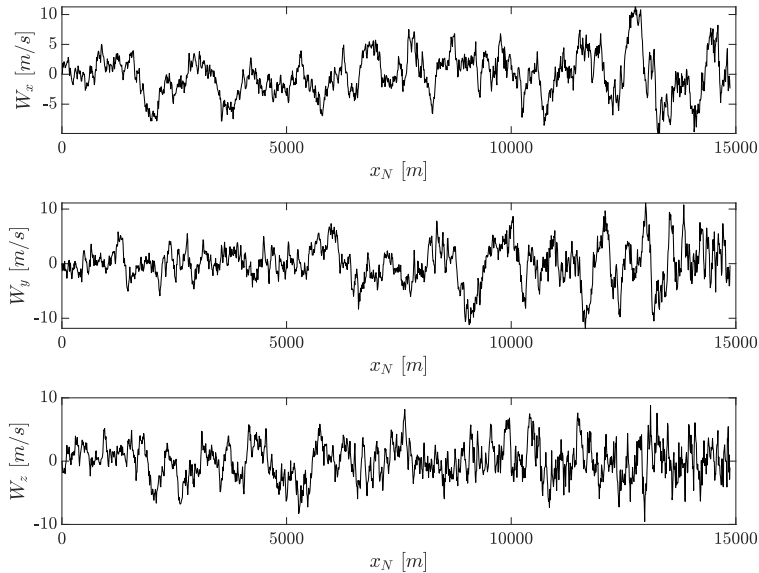


FIGURE 5. The wind components W_x [m/s], W_y [m/s], and W_z [m/s] in the case of a Dryden disturbance model with the characteristic value of 30 m/s.

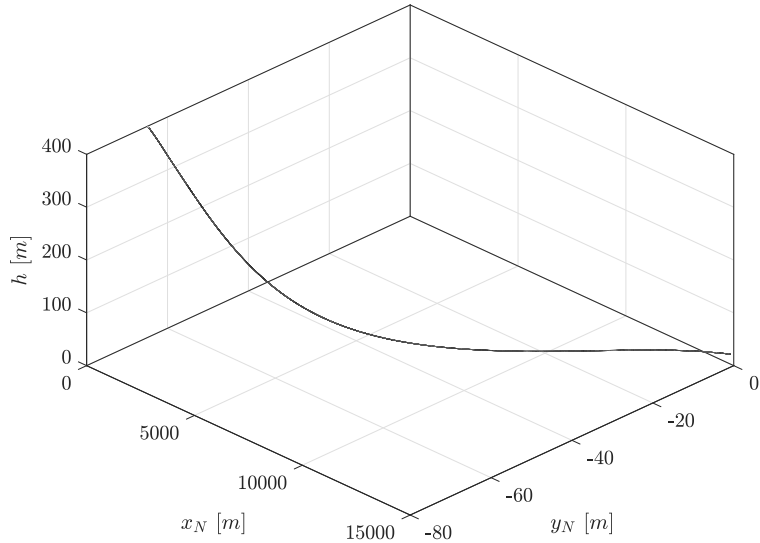


FIGURE 6. Tracking of the landing trajectory in the case of a Dryden disturbance model with the characteristic value of 45 m/s. The black line presents the aircraft motion, and the grey line shows the reference trajectory.

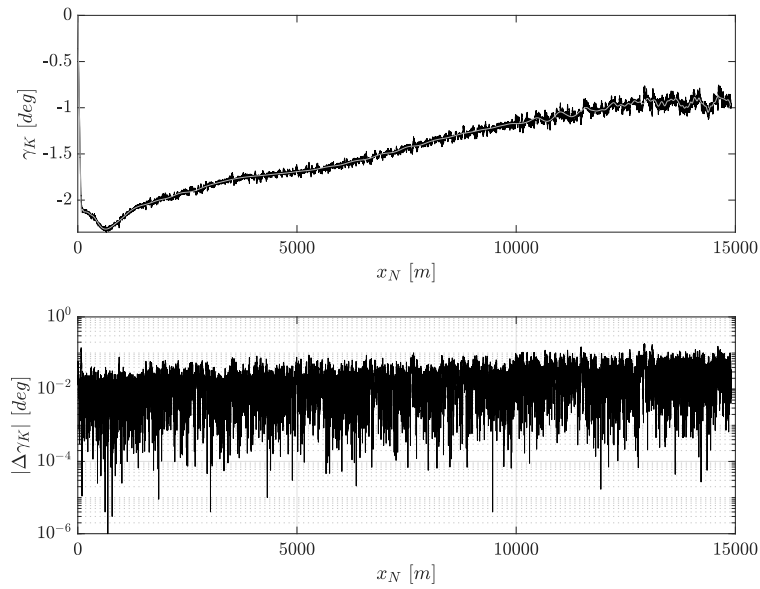


FIGURE 7. The angle γ_K [deg] in the case of a Dryden disturbance model with the characteristic value of 45 m/s. In the upper plot the black line corresponds to the aircraft motion, and the grey line stands for the reference trajectory. The solid line in the lower plot shows the absolute tracking error using a semi-logarithmic scale.

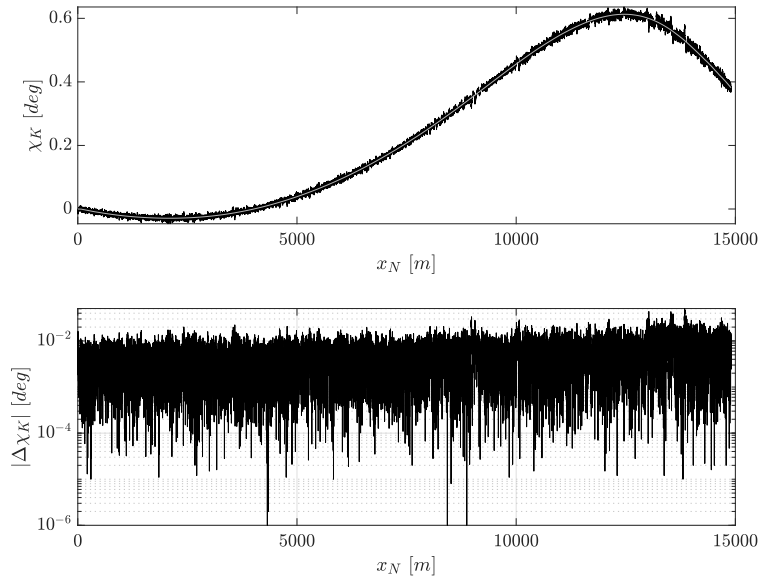


FIGURE 8. The angle χ_K [deg] in the case of a Dryden disturbance model with the characteristic value of 45 m/s. In the upper plot the black line corresponds to the aircraft motion, and the grey line stands for the reference trajectory. The solid line in the lower plot shows the absolute tracking error using a semi-logarithmic scale.

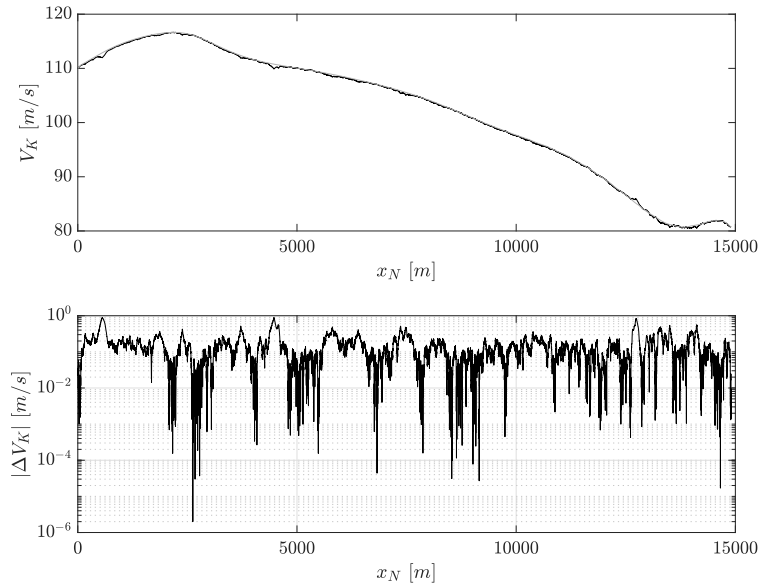


FIGURE 9. The velocity V_K [m/s] in the case of a Dryden disturbance model with the characteristic value of 45 m/s. In the upper plot the black line corresponds to the aircraft motion, and the grey line stands for the reference trajectory. The solid line in the lower plot shows the absolute tracking error using a semi-logarithmic scale.

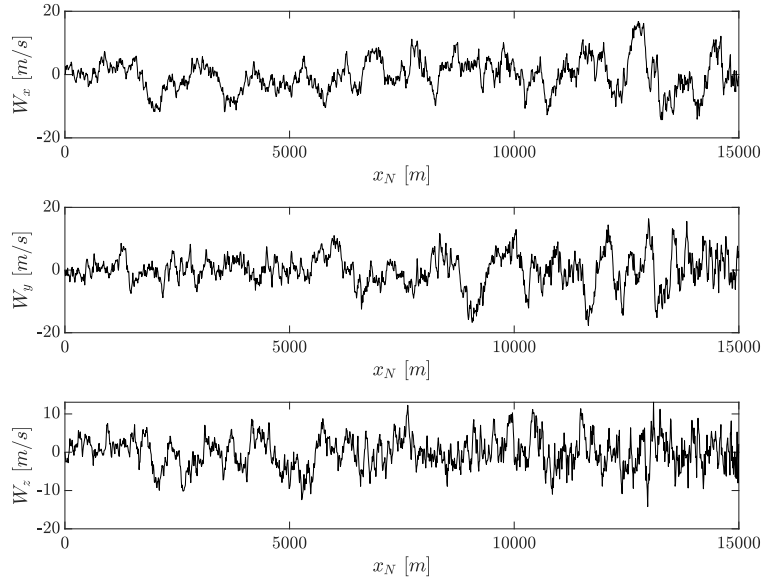


FIGURE 10. The wind components W_x [m/s], W_y [m/s], and W_z [m/s] in the case of a Dryden disturbance model with the characteristic value of 45 m/s.

6.2. Tracking a cruise flight trajectory. A point-mass model describing the dynamics of a generic modern transport aircraft is considered. This model is carefully presented in paper [2] (the only difference is that the kinematic angle of side-slip is not a control input there), so that it is not necessary to repeat its derivation. The state vector of the model is $x = [V_K, \gamma_K, \chi_K, x_N, y_N, z_N]'$, where V_K is the kinematic velocity, γ_K the kinematic inclination angle, χ_K the kinematic course angle, and (x_N, y_N, z_N) represent the position states in a local coordinate system.

On the one side, the vector of control inputs $u = [\alpha_K, \beta_K, \mu_K, \delta_T]'$ collects the kinematic angle of attack α_K , the kinematic angle of slide-slip β_K , the kinematic bank angle μ_K , and the thrust setting δ_T . On the other side, the wind velocity components W_x , W_y , and W_z are regarded as disturbances. These controls and disturbances are bounded by

$$\begin{aligned} |\alpha_K| \leq 15 \text{ deg}, \quad |\beta_K| \leq 5 \text{ deg}, \quad |\mu_K| \leq 5 \text{ deg}, \quad \delta_T \in [0.3, 1], \\ |W_x| \leq 10 \text{ m/s}, \quad |W_y| \leq 10 \text{ m/s}, \quad |W_z| \leq 5 \text{ m/s}, \end{aligned} \quad (37)$$

and the manifold to be tracked (reference trajectory) is given as:

$$V_K = 150 \text{ m/s}, \quad \gamma_K = 0 \text{ deg}, \quad \chi_K = 0 \text{ deg}, \quad y_N = 0 \text{ deg}, \quad z_N = -5000 \text{ m}.$$

It is numerically proven that the saddle point condition does not hold, so that the control scheme corresponds to Subsection 4.3. The saddle point condition is evaluated on the reference trajectory in the same way as described in the first numerical example. The choice of the controls $u^{(i)}(t)$ in the guide model is implemented according to the ansatz (29) and (30). Moreover, disturbances are simulated as repulsive pushes defined by formula (25). For this example the controls in Alg. 1 are not computed in a sequential manner as it was done in the first example due to the fact that the reference velocity is held constant. The time step lengths $\delta = 0.005$ s

and $\tau = 0.05$ s are chosen and the state vector of the guide model (see Remark 2) is reset with the threshold $\epsilon_0 = 0.01$. The simulations are performed on the time interval of 100 s. The runtime is about 150 s with OMP parallelization over 11 threads. It should be noted that stable tracking appears to hold for any time interval (tested up to 3600 s). The simulation results are depicted in Figures 11-15.

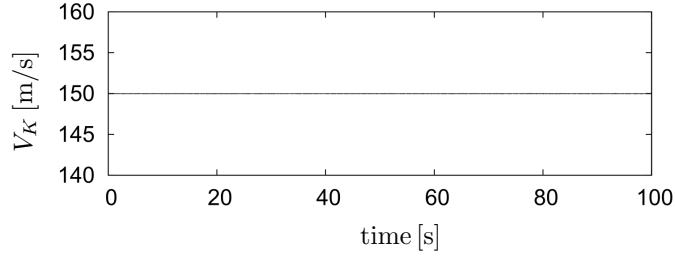


FIGURE 11. The kinematic velocity V_K [m/s] for the case of repulsive disturbance, see (24). The straight line at $V_K = 150$ m/s corresponds to the reference.

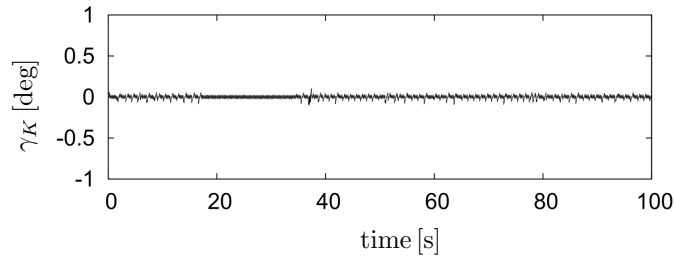


FIGURE 12. The angle γ_K [deg] for the case of repulsive disturbance, see (24). The straight line at $\gamma_K = 0$ deg corresponds to the reference.

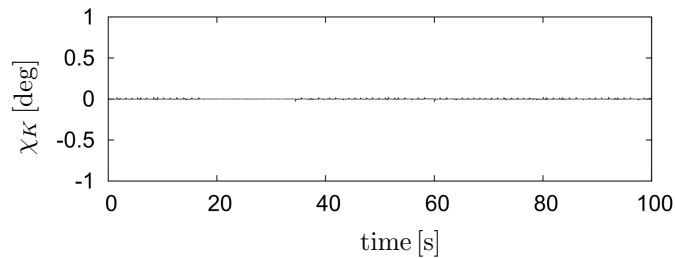


FIGURE 13. The angle χ_K [deg] for the case of repulsive disturbance, see (24). The straight line at $\chi_K = 0$ deg corresponds to the reference.

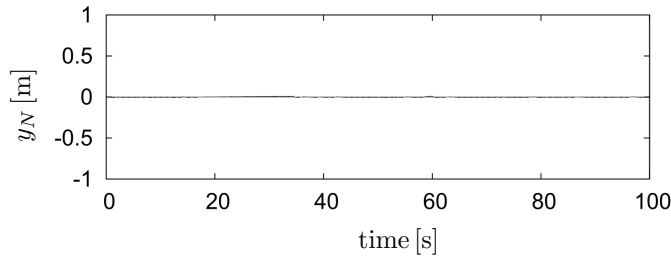


FIGURE 14. The position component y_N [m] for the case of repulsive disturbance, see (24). The straight line at $y_N = 0$ m corresponds to the reference.

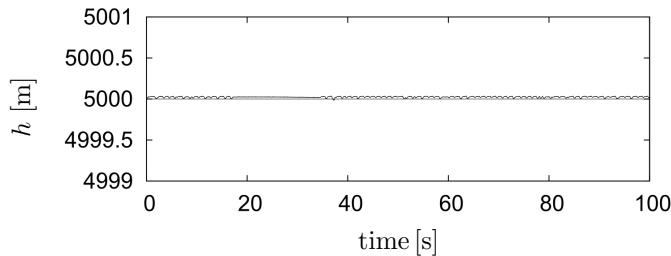


FIGURE 15. The altitude $h = -z_N$ [m] for the case of repulsive disturbance, see (24). The straight line at $h = 5000$ m corresponds to the reference.

7. Conclusion. The examples presented in this paper show that the differential game based tracking method can be applied to the aircraft trajectory following task under rather severe and unpredictable windshear conditions. It should be stressed that the current choice of control is only based on the current state of the aircraft and a measurement of the wind disturbance is not required. The drawback of the method is that the resulting controls are of bang-bang type with very frequent switches. In this context, it is important to mention that the control inputs of point-mass models are in fact states of full aircraft models which are controlled by the primary control surfaces such as the aileron, rudder, and elevator. In order to apply the controls obtained from a point-mass model under the approach proposed in this paper to the full model the principle of nonlinear dynamic inversion [20] may be used in order to restore the actuator signals based on the resulting (smoothed) trajectory. A similar idea has been implemented by the authors (see [8]) in the context of tracking controls computed from a point-mass model by solving appropriate Hamilton-Jacobi equations.

8. Appendix.

8.1. Model Dynamics. A nonlinear point mass model of the Boeing 707 jet is under consideration. Conventional notations for reference frames, see [10] and [3], are used. Matrices defining the transformations between reference frames are described in Subsection 8.3. Here, it should be mentioned that the kinematic angle of

sideslip β_K of the aircraft is assumed to be zero and the corresponding rotation is, as such, neglected in all transformation matrices.

The dynamic equations of the aircraft read as follows:

$$\begin{aligned}\dot{V}_K &= \frac{1}{m} [X_K - mg \sin(\gamma_K)], \\ \dot{\gamma}_K &= -\frac{1}{mV_K} [Z_K + mg \cos(\gamma_K)], \\ \dot{\chi}_K &= \frac{1}{mV_K \cos(\gamma_K)} Y_K, \\ \dot{x}_N &= V_K \cos(\gamma_K) \cos(\chi_K), \\ \dot{y}_N &= V_K \cos(\gamma_K) \sin(\chi_K), \\ \dot{z}_N &= -V_K \sin(\gamma_K).\end{aligned}$$

In these equations, m is the aircraft mass, g the gravitational acceleration, V_K the kinematic velocity, γ_K the kinematic flight path angle, χ_K the kinematic azimuth angle, and (x_N, y_N, z_N) the aircraft position in a local reference frame. Moreover, X_K , Y_K , and Z_K are components of the sum of aerodynamic and propulsion forces in the kinematic frame:

$$\begin{bmatrix} X_K \\ Y_K \\ Z_K \end{bmatrix} = (\mathbf{F}_A)_K + (\mathbf{F}_P)_K.$$

The aerodynamic force $(\mathbf{F}_A)_K$ denoted in the kinematic frame is defined as

$$(\mathbf{F}_A)_K = \mathbf{M}_{KB}(\mu_K, \alpha_K) \mathbf{M}_{BA}(\alpha_A, \beta_A) \begin{bmatrix} -C_D \bar{q} \\ C_{Y\beta} \beta_A \bar{q} \\ -C_L \bar{q} \end{bmatrix}, \quad (38)$$

with the drag coefficient C_D , the side-force coefficient $C_{Y\beta}$, and the lift coefficient C_L . The matrix \mathbf{M}_{KB} represents the transformation matrix from the body-fixed to the kinematic reference frame and depends on the kinematic angle of attack α_K and the kinematic bank angle μ_K . Moreover, the matrix \mathbf{M}_{BA} denotes the transformation matrix between the aerodynamic and the body-fixed frame depending on the aerodynamic angle of sideslip β_A and the aerodynamic angle of attack α_A . These two aerodynamic angles are computed based on the formulas

$$\begin{aligned}\alpha_A &= \arctan \left(\frac{(w_A)_B}{(u_A)_B} \right), \\ \beta_A &= \arctan \left(\frac{(v_A)_B}{\sqrt{(u_A)_B^2 + (w_A)_B^2}} \right),\end{aligned}$$

where $(u_A)_B$, $(v_A)_B$ and $(w_A)_B$ are the components of the aerodynamic velocity $(\mathbf{V}_A)_B = [(u_A)_B, (v_A)_B, (w_A)_B]'$ in the body-fixed frame. The propulsion force vector is obtained as

$$(\mathbf{F}_P)_K = \mathbf{M}_{KB}(\mu_K, \alpha_K) \begin{bmatrix} \delta_T T_{max} \\ 0 \\ 0 \end{bmatrix}, \quad (39)$$

under the assumption that the propulsion force of the aircraft is aligned with the x_B -axis of the body-fixed frame.

Furthermore, the dynamic pressure \bar{q} in equation (38) is defined as

$$\bar{q} = \frac{1}{2}\rho V_A^2, \quad V_A = \|(\mathbf{V}_K)_O - (\mathbf{V}_W)_O\|, \quad (40)$$

with the kinematic velocity $(\mathbf{V}_K)_O = \mathbf{M}_{OK}(\chi_K, \gamma_K)[V_K, 0, 0]'$ and the wind velocity $(\mathbf{V}_W)_O$, both denoted in the NED frame. The matrix \mathbf{M}_{OK} represents the transformation matrix from the kinematic frame (K) to the NED frame (O) and depends on the kinematic course angle χ_K as well as the kinematic climb angle γ_K .

It is assumed that the air density ρ varies with the altitude h according to the International Standard Atmosphere (ISA), as described in [6] for the troposphere layer. In the current work, the air density is set to 1.0581 kg m^{-3} at the altitude $h = 400 \text{ m}$.

The lift and drag coefficients are of the form

$$C_L = C_{L_0} + \alpha_A C_{L_\alpha}, \quad C_D = C_{D_0} + \alpha_A C_{D_\alpha},$$

and the values of the aerodynamic parameters C_{D_0} , C_{D_α} , C_{L_0} , C_{L_α} , C_{Y_β} , as well as other model data corresponding to the landing configuration, can be found in [5]. Increased values of C_{L_0} and C_{D_0} reflect the effects of the configuration of the aircraft during the landing phase.

The variable T_{max} , appearing in equation (39), denotes the maximum thrust produced by the engines at the current velocity and altitude, whereas $\delta_T \in [0, 1]$ is the thrust setting. Depending on the flight condition, the maximum thrust T_{max} is given by the equation

$$T_{max} = T_{maxref} \left(\frac{V_A}{V_{Aref}} \right)^{n_V} \left(\frac{\rho_h}{\rho_{ref}} \right)^{n_\rho}, \quad (41)$$

where n_V and n_ρ are empirical values corresponding to the engine type. The ansatz (41) and the values $n_V = -0.1$ and $n_\rho = 0.7$ are chosen based on the methods described in [6] for turbofan engines with a low bypass ratio. The other parameters are chosen as $\rho_{ref} = 1.0581 \text{ kg m}^{-3}$, $V_{Aref} = 130 \text{ m s}^{-1}$, and $T_{maxref} = 320800 \text{ N}$.

Summarizing, the state and control vectors of the aircraft model are defined as $x = [V_K, \gamma_K, \chi_K, x_N, y_N, z_N]'$ and $u = [\alpha_K, \mu_K, \delta_T]'$. Moreover, the disturbances are represented by the components of the vector $(\mathbf{V}_W)_O$, i.e. the wind velocities denoted in the NED frame.

8.2. Dryden Disturbance Model. In order to generate realistic wind disturbances along the landing trajectory, the Dryden turbulence model (see [7]) is utilized. Roughly speaking, this model applies an adaptive filter on band-limited white noise to generate disturbances that take eigenfrequencies of the aircraft dynamics into account. This model is considered because these wind disturbances are deemed more realistic compared to e.g. a constant wind field, purely random signals or repulsive gusts defined by (24). It is important to mention that only turbulence velocities are considered in our study, whereas the turbulence angular rates are neglected.

For the Dryden model, the wind velocity at 6 m represents the characteristic value of the turbulence intensity in lower altitudes (under 1000 ft). In the present study, the values of 30 m/s and 45 m/s are considered for the low altitude intensity.

8.3. Transformation matrices. In order to define the transformation matrices used for the flight mechanical model it is useful to introduce the following elementary

rotation matrices around the x -, y -, and z -axis for a generic angle ϕ :

$$\mathbf{M}_x(\phi) = \begin{bmatrix} 1 & 0 & 0 \\ 0 & \cos(\phi) & \sin(\phi) \\ 0 & -\sin(\phi) & \cos(\phi) \end{bmatrix},$$

$$\mathbf{M}_y(\phi) = \begin{bmatrix} \cos(\phi) & 0 & -\sin(\phi) \\ 0 & 1 & 0 \\ \sin(\phi) & 0 & \cos(\phi) \end{bmatrix},$$

$$\mathbf{M}_z(\phi) = \begin{bmatrix} \cos(\phi) & \sin(\phi) & 0 \\ -\sin(\phi) & \cos(\phi) & 0 \\ 0 & 0 & 1 \end{bmatrix}.$$

Based on these definitions the transformation matrices appearing in the model description can be composed as follows:

$$\mathbf{M}_{OK} = \mathbf{M}_z(-\chi_K) \mathbf{M}_y(-\gamma_K), \quad (42)$$

$$\mathbf{M}_{BA} = \mathbf{M}_y(\alpha_K) \mathbf{M}_z(-\beta_A), \quad (43)$$

$$\mathbf{M}_{BK} = \mathbf{M}_y(\alpha_K) \mathbf{M}_x(\mu_K). \quad (44)$$

For the construction of the transformation matrix \mathbf{M}_{BK} the rotation with the kinematic angle of side-slip β_K is neglected as this angle is assumed zero.

REFERENCES

- [1] J. T. Betts, *Practical Methods for Optimal Control and Estimation Using Nonlinear Programming*, Advances in Design and Control, 19. Society for Industrial and Applied Mathematics (SIAM), Philadelphia, PA, 2010.
- [2] N. Botkin, J. Diepolder, V. Turova, M. Bittner and F. Holzapfel, *Viability approach to aircraft control in windshear conditions*, in *Advances in Dynamic and Mean Field Games* (eds. J. Apaloo and B. Viscolani), Birkhäuser, (2017), 325–343.
- [3] N. Botkin, V. Turova, J. Diepolder, M. Bittner and F. Holzapfel, *Aircraft control during cruise flight in windshear conditions: Viability approach*, *Dynamic Games and Applications*, **7** (2017), 594–608.
- [4] H. Bouadi and F. Mora-Camino, *Aircraft trajectory tracking by nonlinear spatial inversion*, in *AIAA Guidance, Navigation, and Control Conference*, Minneapolis, Minnesota, August (2012), 13–16.
- [5] R. Brockhaus, W. Alles and R. Luckner, *Flugregelung*, Springer, 2011.
- [6] G. Brüning, X. Hafer and G. Sachs, *Flugleistungen*, 2nd edition, Springer, 1986.
- [7] C. R. Chalk, T. P. Neal, T. M. Harris, F. E. Pritchard and R. J. Woodcock, *Background Information and User Guide for Mil-F-8785B (ASG)*, ‘Military Specification-Flying Qualities of Piloted Airplanes’, Cornell Aeronautical Lab Inc Buffalo Ny, 1969.
- [8] J. Diepolder, P. Piprek, N. Botkin, V. Turova and F. Holzapfel, *A robust aircraft control approach in the presence of wind using viability theory*, in *2017 Australian and New Zealand Control Conference (ANZCC)*, IEEE, (2017), 155–160.
- [9] A. Farooq and D. J. N. Limebeer, *Path following of optimal trajectories using preview control*, in *Proceedings of the 44th IEEE Conference on Decision and Control*, Seville, Spain, (2005), 2787–2792.
- [10] F. Fisch, *Development of a Framework for the Solution of High-Fidelity Trajectory Optimization Problems and Bilevel Optimal Control Problems*, Ph.D. thesis, Chair of Flight System Dynamics, Technical University of Munich, 2011.
- [11] N. N. Krasovskii and A. I. Subbotin, *Game-Theoretical Control Problems*, Springer-Verlag, New York, 1988.
- [12] Y. S. Osipov and A. V. Kryazhimskiy, *Inverse Problems for Ordinary Differential Equations: Dynamical Solutions*, Gordon and Breach Science Publishers, Basel, 1995.
- [13] A. V. Kryazhimskiy and V. I. Maksimov, *Resource-saving tracking problem with infinite time horizon*, *Differential Equations*, **47** (2011), 1004–1013.

- [14] A. V. Kryzhinskii and V. I. Maksimov, [On combination of the processes of reconstruction and guaranteeing control](#), *Automation and Remote Control*, **74** (2013), 1235–1248.
- [15] G. Leitmann, S. Pandey and E. Ryan, [Adaptive control of aircraft in windshear](#), *Int. Journal of Robust and Nonlinear Control*, **3** (1993), 133–153.
- [16] I. Lugo-Cárdenas, S. Salazar and R. Lozano, [Lyapunov based 3D path following kinematic controller for a fixed wing UAV](#), in *IFAC-PapersOnLine*, **50** (2017), 15946–15951.
- [17] V. I. Maksimov, [The tracking of the trajectory of a dynamical system](#), *J. Appl. Math. Mech.*, **75** (2011), 667–674.
- [18] V. I. Maksimov, [Differential guidance game with incomplete information on the state coordinates and unknown initial state](#), *Differential Equations*, **51** (2015), 1656–1665.
- [19] A. Miele, T. Wang and W. W. Melvin, [Optimization and gamma/theta guidance of flight trajectories in a windshear](#), in *ICAS, Congress, 15th*, London, England, September 7-12, 1986, Proceedings Volume 2, 878–899.
- [20] J. -J. E. Slotine and W. Li, *Applied Nonlinear Control*, Taipei : Prentice Education Taiwan Ltd., 2005.
- [21] A. Wächter and L. T. Biegler, [On the implementation of a primal-dual interior point filter line search algorithm for large-scale nonlinear programming](#), *Mathematical Programming*, **106** (2006), 25–57.

Received March 2019; revised July 2020.

E-mail address: botkin@ma.tum.de

E-mail address: turova@ma.tum.de

E-mail address: barzin.hosseini@tum.de

E-mail address: johannes.diepolder@tum.de

E-mail address: florian.holzapfel@tum.de